Direct Assembly of Photoresponsive C_{60}–Gold Nanoparticle Hybrid Films

Tuong Dinh and Young-Seok Shon*

Department of Chemistry and Biochemistry, California State University at Long Beach, 1250 Bellflower Boulevard, Long Beach, California 90840

ABSTRACT The C_{60}–gold nanoparticle hybrid films prepared by the in situ cross-linking assembly have smoother and more featureless surfaces than the films generated by the layer-by-layer assembly. The electrical properties of these novel nanostructures are also strongly dependent upon the film assembly methods. The hybrid films prepared by the in situ cross-linking assembly are found to be very sensitive to UV illumination. The films responded with a decrease in the current upon exposure, followed by a recovery of the current upon removal of the UV lights.

KEYWORDS: nanoparticle • nanostructure • fullerene • photodetector • assembly

INTRODUCTION

There have been increased research interests directed at using colloidal semiconductor nanoparticles as active components in photodetectors (1–4). This is largely due to their solution processability, which helps to eliminate the vacuum and high-temperature processes required for conventional semiconductor processing and reduce the overall cost of device fabrication. However, many recent advances in semiconductor nanoparticle-based photodetectors have relied on the use of heavy metals such as Cd and Pb, which raise environmental regulatory concerns (1–4). Recently, heavy-metal-free systems such as Bi_2S_3 (5), In_2S_3 (6), and ZnO (7, 8) nanoparticles have also been explored as the photoactive layer in conductive photodetectors. However, either the synthesis or the preparation of photoactive layers based on these nanoparticles required an inert atmosphere or high-temperature processing.

Gold nanoparticle- or fullerene-based materials have offered the ability to tune component properties through the careful assembly of either material as a building block. In addition, their lower chemical toxicity has been the driving force for the increased interest on device applications using both nanomaterials individually or together (9). Fullerenes, which possess relatively high electron affinity and large numbers of π orbitals, are known to have good charge-transfer properties and confer promising electronic properties (10–12). Combining these properties of fullerenes with the interesting quantum-dot-like properties of ligand-stabilized gold nanoparticles has offered a potential for applications to the photonic and molecular electronic devices (13, 14).

We herein report a simple and inexpensive approach to the direct assembly of hybrid films consisting of fullerene (C_{60}) and novel gold nanoparticles (~2 nm) onto interdigitated microelectrodes (IDEs) via self-assembly and a demonstration of the photodetector device capability of this hybrid system. The direct self-assembly method that we use provides an opportunity to create devices under ambient conditions without the use of expensive instruments (9).

EXPERIMENTAL METHODS

We targeted the preparation of controlled assemblies using both the layer-by-layer (LbL) (15) and the in situ cross-linking assembly methods to fine-tune the structure of C_{60}–gold nanoparticle hybrid nanostructures (Figure 1). The driving force for the formation of C_{60}–gold nanoparticle hybrid films was the amination reaction of C_{60} with amine-functionalized gold nanoparticles (15–17). In addition, we prepared the drop-casted films of C_{60} and C_{60}-conjugated gold nanoparticle (15, 16) films on IDEs and used them as references. The C_{60} and C_{60}-conjugated gold nanoparticle films were cast onto the IDEs from several drops (until conductivities were identical) of a toluene solution (0.1 mL) containing either ~5 mg of C_{60} or ~5 mg of nanoparticles (18, 19).

To build the C_{60}–gold nanoparticle hybrid films, the solid substrates were functionalized with (3-aminopropyl)trimethoxysilane (see the Supporting Information for details). Gold surfaces of IDEs were further treated with 2-aminoethanolthiol for the direct immobilization of C_{60} (16).

For the LbL assembly, the functionalized glass slides or IDEs were alternately soaked in solutions containing unmodified C_{60} (1 mg/mL) and 4-aminothiophenoxide/hexanethiolate-protected gold nanoparticles (1 mg/mL) (15). On the basis of our previous results, the self-assembly of each C_{60} and gold nanoparticle layer requires more than 2 days for reasonable coverage of the film surfaces (15). The C_{60}–gold nanoparticle hybrid films have grown up to five bilayers by this approach.

For the in situ cross-linking assembly (20), the substrates were immersed in the solution containing both C_{60} and 4-aminothiophenoxide/hexanethiolate-protected gold nanoparticles for 24 h. The thickness of the in situ assembly was dependent upon the immersion time of the solid substrates in the solution.

RESULTS AND DISCUSSION

Both C_{60}–gold nanoparticle hybrid films prepared on glass substrates by the LbL assembly and the in situ cross-linking assembly methods were monitored using UV–vis

* Corresponding author footnote. E-mail: yshon@csulb.edu.
Received for review August 14, 2009 and accepted November 12, 2009

DOI: 10.1021/am900548k

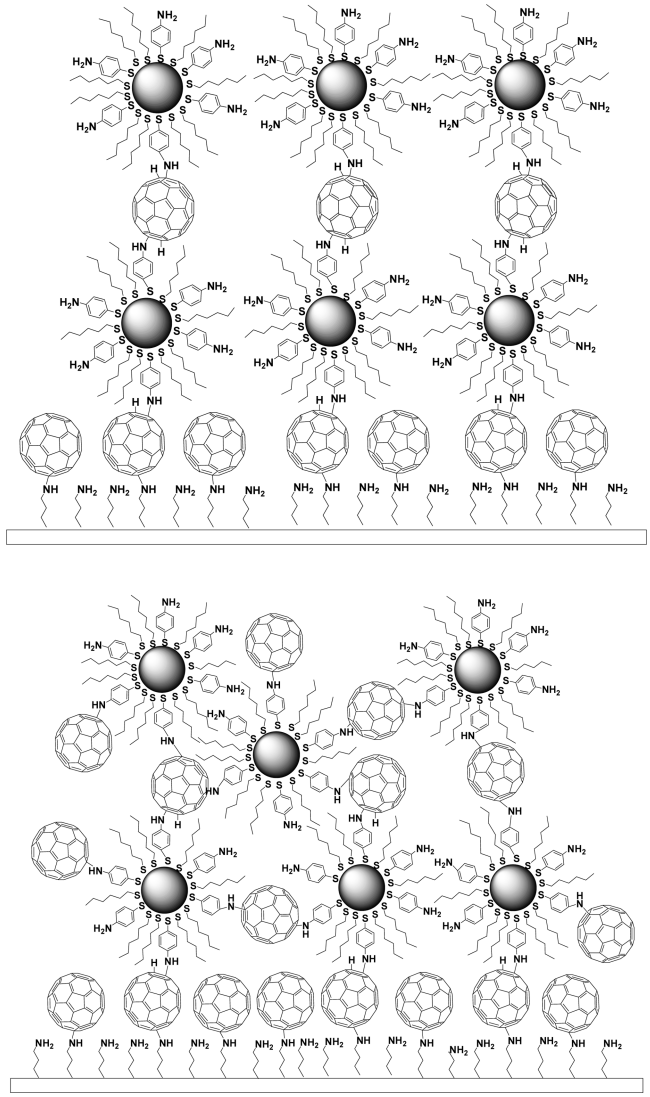

FIGURE 1. Cartoons of C_{60}–gold nanoparticle hybrid films assembled by the LbL (above) and the in situ cross-linking assembly (below).

spectroscopy (Figure 2). These results showed that the surface plasmon band of gold at ~545 nm gradually became more evident as more nanoparticle layers were added to the films. It has been found that the in situ cross-linking assembly generates films of comparable thicknesses in a shorter time (~24 h) compared to the LbL assembly (20 days).

The LbL films are expected to have mostly "bottom-to-top" connections between C_{60} and gold nanoparticles considering the intrinsic characteristics of the deposition protocol. In comparison, the in situ cross-linking assembled films should have more complex "side-to-side" connections in addition to "bottom-to-top" connections. Presumably, these structural differences of the hybrid films would have some influence over the overall electrical property of the films.

Both assemblies were characterized using atomic force microscopy (AFM). The hybrid films prepared by the in situ assembly have smoother and more featureless surfaces (see Figure S1 in the Supporting Information). In contrast, the hybrid films prepared by the LbL assembly have course and rough surfaces. This is simply due to the characteristics of the in situ cross-linking assembly that can fill up the defect sites of the films during the self-assembly process. AFM can also provide viable information on the thickness of nanostructured films by determining the average height differences between the assembled films and the uncovered (defected) surface. Analysis of the film heights suggested that the average thickness of the LbL films was ca. 25 nm. For the in situ cross-linked films, the average AFM-measured height was ca. 22 nm.

Electrical properties of the hybrid films deposited on IDEs were also measured for both assembly types using surface tunneling spectroscopy (STS; see Figure S2 in the Supporting Information). Reflecting the smoother and more consistent surface, a linear relationship for the current–potential response was observed for the in situ cross-linked assembly. Films prepared via the LbL assembly showed an inconsistent trend, indicating that the surface is not as conductive as the films generated by the in situ cross-linking assembly. This indicated that the LbL films might not be fully and completely connected.

Table 1 summarizes the electrical conductivity obtained from cyclic voltammetry (linear potential sweep) results of each film, including drop-casted films and self-assembled films, in the dark (see Figure S3 in the Supporting Information). Analysis of the hybrid films using cyclic voltammetry confirmed that the LbL hybrid film has a very low conductivity, whereas the in situ cross-linking assembly has a relatively high conductivity. The lack of "side-to-side" connectivity of the LbL-assembled films might have an important role on such electrical behavior. These results suggested that the preparation of photoactive layers by the in situ cross-linking assembly would promote the better overall electrical property of the hybrid films.

When the hybrid films were exposed to UV light with a wavelength of 365 nm in dark conditions, a trend reminiscent of a current inhibition was observed for the in situ cross-linking assembly films. As shown in Figure 3a, the significant current decrease occurs during the first 80 min of UV illumination. No other films consisting of C_{60} or gold nanoparticles studied here exhibited this kind of response to UV light, suggesting the importance of chemical-bonding patterns in the films. The results showed that, as the amount of time under UV light was increased, the current passing through the nanoparticle hybrid films generated from the in situ cross-linking assembly decreased asymptotically. The characteristic current inhibition graph could fit to the kinetic equation $y = y_0 + ae^{-bx}$ ($y_0 = -7.07 \times 10^{-3}$, $a = 7.45 \times 10^{-3}$, and $b = 2.35 \times 10^{-2}$).

The reequilibration time of the hybrid films and its responsiveness were also investigated. The film was exposed to UV light at constant intervals (except one at ~250 s with an extra 10 s of exposure) of 30 s (Figure 3b). The in situ cross-linking assembly films responded with a current decrease to the UV exposure, followed by a current recovery to the removal of the lights. Each time the film was irradiated in this manner, sharp and distinct peaks were observed. All

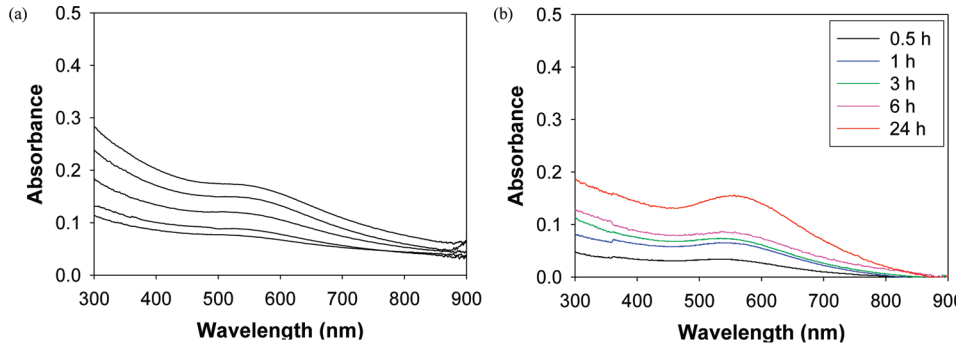

FIGURE 2. UV−vis spectra of C_{60}−gold nanoparticle hybrid films assembled by (a) the LbL assembly method and (b) the in situ cross-linking assembly method.

Table 1. Conductivity Data and Current Response of C_{60} and C_{60}−Gold Nanoparticle (NP) Hybrid Films

film	$d\Delta I/A_{total}\Delta E$ ($\Omega^{-1}cm^{-1}$; σ_{EL})[a]	$\Delta I_t/I_0$ (t = 30 s)
drop-casted C_{60}	3.10×10^{-2}	0
drop-casted gold NPs	1.42×10^{-1}	
drop-casted C_{60}−gold NPs	3.35×10^{-2}	0
LbL-assembled C_{60}−gold NPs	6.63×10^{-6}	0
in situ assembled C_{60}−gold NPs	3.91×10^{-2}	-2.77×10^{-4}

[a] From the linear potential sweeps of the different films (d and A_{total} are the gap distance and the total electrode area of IDE, respectively).

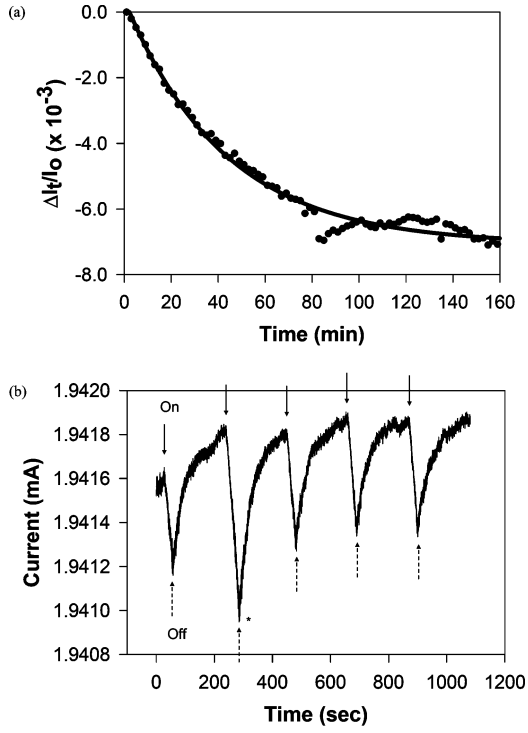

FIGURE 3. Current response of C_{60}−gold nanoparticle hybrid films assembled by the in situ cross-linking assembly upon exposure to UV (365 nm). (*) At approximately 250 s in graph b, the intensity of the current decrease was higher as a result of the additional exposure time (10 s more) under UV light.

peaks remained fairly similar in intensity after every 30 s of UV exposure. The average current decrease was calculated and is listed in Table 1. The time it took for the film to return to its normal current state was observed to be approximately 120 s after 30 s of exposure.

No other films including the drop-casted C_{60} films (no C_{60}−NH_2 bonds), the C_{60}-conjugated gold nanoparticle films (localized C_{60}−NH_2 bonds), and the LbL films (two-dimensionally oriented C_{60}−NH_2 bonds) responded to the UV exposure (see Figure S4 in the Supporting Information). These results suggested that the extensive cross-linking of C_{60} with amine-functionalized gold nanoparticles (three-dimensionally oriented C_{60}−NH_2 bonds) is important for the photoresponsive characteristics of C_{60}−gold nanoparticle hybrid films. Because gold nanoparticles serve as a platform for multiple C_{60} conjugation with reactive amine ligands around the nanoparticle core, the presence of amine-functionalized gold nanoparticles during the in situ assembly allows cross-linking of C_{60} and gold nanoparticles. On the basis of the AFM and STS results, the electrical conductivity and surface morphology of the films are also closely related. Therefore, both chemical bonding and morphology of the films should have influence over the photoresponsive characteristics of the films.

The current decrease is likely due to the combination of photons from UV light interacting with C_{60}[21] in the hybrid film and subsequent charge trapping caused by the absorbance of photons. This charge trapping then reduces the flow of current across the film and causes a decrease in the conductivity. Some of the possible charge-trapping mechanisms that are known include conversion of free charges into immobile bipolarons, stabilization by dipoles in dielectric layers, charge migration into dielectric layers, and chemical reactions with impurities (22). The current decrease upon exposure to UV light is quite unique considering that the current increase generally takes place for other photodetector systems by UV illumination (1−6). The detailed mechanism of charge trapping that occurs for this hybrid film will be a focal point of future studies.

CONCLUSION

The C_{60}−gold nanoparticle hybrid films were prepared by both the in situ cross-linking assembly and the LbL assembly. Our system does not rely on the use of heavy metals and does not require an inert atmosphere or high-temperature processing. The creation of photosensitive device arrays based on the C_{60}−gold nanoparticles was, therefore, achieved entirely under ambient conditions. The hybrid films prepared by the in situ cross-linking assembly had smoother

and more featureless surfaces than the films generated by the LbL assembly. The electrical properties of these novel nanostructures were also strongly dependent upon the film assembly methods. The in situ cross-linking assembly films were more conductive than those films prepared by the LbL assembly. Additionally, the in situ cross-linking assembly films were found to be sensitive to the presence of UV lights. The films responded with a decrease in the current upon exposure, followed by a recovery of the current upon removal of the UV lights. We anticipate that the understanding of electron/charge-transfer and photochemical properties of a well-designed C_{60}–gold nanoparticle assembly will provide a tremendous opportunity for applications in the optics and electronics fields.

Acknowledgment. This research was partially supported by grants from the American Chemical Society (ACS-PRF) and California State University at Long Beach.

Supporting Information Available: Procedure for the preparation of C_{60}–gold nanoparticle hybrid films on glass slides and IDEs and characterization results including AFM images, STS results, cyclic voltammograms, and additional i–t graphs. This material is available free of charge via the Internet at http://pubs.acs.org.

REFERENCES AND NOTES

(1) Amos, F. F.; Morin, S. A.; Streifer, J. A.; Hamers, R. J.; Jin, S. *J. Am. Chem. Soc.* **2007**, *129*, 14296–14302.
(2) Jarosz, M. V.; Porter, V. J.; Fisher, B. R.; Kastner, M. A.; Bawendi, M. G. *Phys. Rev. B* **2004**, *70*, 19532.
(3) Murphy, J. E.; Beard, M. C.; Nozik, A. J. *J. Phys. Chem. B* **2006**, *110*, 25455–25461.
(4) Yong, K.-T.; Sahoo, Y.; Choudhury, K. R.; Swihart, M. T.; Minter, J. R.; Prasad, P. N. *Chem. Mater.* **2006**, *18*, 5965–5972.
(5) Tang, J.; Konstantatos, G.; Hinds, S.; Myrskog, S.; Pattantyus-Abraham, A. G.; Clifford, J.; Sargent, E. H. *ACS Nano* **2009**, *3*, 331–338.
(6) Konstantatos, G.; Levina, L.; Tang, J.; Sargent, E. H. *Nano Lett.* **2008**, *8*, 4002–4006.
(7) Jin, Y.; Wang, J.; Sun, B.; Blakesley, J. C.; Greenham, N. C. *Nano Lett.* **2008**, *8*, 1649–1653.
(8) Zhu, Z.; Zhang, L.; Howe, J. Y.; Liao, Y.; Speidel, J. T.; Smith, S.; Fong, H. *Chem. Commun.* **2009**, 2568–2570.
(9) Claridge, S. A.; Castleman, A. W., Jr.; Khanna, S. N.; Murray, C. B.; Sen, A.; Weiss, P. S. *ACS Nano* **2009**, *3*, 244–255.
(10) Guldi, D. M. *Chem. Commun.* **2000**, 321–327.
(11) Imahori, H.; Azuma, T.; Ajavakom, A.; Norieda, H.; Yamada, H.; Sakata, Y. *J. Phys. Chem. B* **1999**, *103*, 7233–7237.
(12) Yang, J.; Li, L.; Wang, C. *Macromolecules* **2003**, *36*, 6060–6065.
(13) Sudeep, P. K.; Ipe, B. I.; Thomas, K. G.; George, M. V.; Barazzouk, S.; Hotchandani, S.; Kamat, P. V. *Nano Lett.* **2002**, *2*, 29–35.
(14) Shih, S.-M.; Su, W.-F.; Lin, Y.-J.; Wu, C.-S.; Chen, C.-D. *Langmuir* **2002**, *18*, 3332–3335.
(15) Shon, Y.-S.; Choo, H. *Chem. Commun.* **2002**, 2560–2561.
(16) Deng, F.; Yang, Y.; Hwang, S.; Shon, Y.-S.; Chen, S. *Anal. Chem.* **2004**, *76*, 6102–6107.
(17) Backer, S. A.; Suez, I.; Fresco, Z. M.; Rolandi, M.; Fréchet, J. M. *Langmuir* **2007**, *23*, 2297–2299.
(18) Wuelfing, W. P.; Murray, R. W. *J. Phys. Chem. B* **2002**, *106*, 3139–3145.
(19) Wuelfing, W. P.; Green, S. J.; Pietron, J. J.; Cliffel, D. E.; Murray, R. W. *J. Am. Chem. Soc.* **2000**, *122*, 11465–11472.
(20) Leibowitz, F. L.; Zheng, W.; Maye, M. M.; Zhong, C. *J. Anal. Chem.* **1999**, *71*, 5076–5083.
(21) Biebersdorf, A.; Dietmüller, R.; Susha, A. S.; Rogach, A. L.; Poznyak, S. K.; Talapin, D. V.; Weller, H.; Klar, T. A.; Feldmann, J. *Nano Lett.* **2006**, *6*, 1559–1563.
(22) Jaquith, M.; Muller, E. M.; Marohn, J. A. *J. Phys. Chem. B* **2007**, *111*, 7711–7714.

AM900548K